

Prostate Helical Tomotherapy: A semi-empirical estimation of the scaling factor based on 2D approximating field

G. Grigorov^{1*} and J.C.L. Chow²

¹Medical Physics Department, Grand River Regional Cancer Center, Kitchener, ON, Canada

²Radiation Medicine Program, Princess Margaret Hospital, Toronto, ON, Canada

Background: In Helical Tomotherapy (HT), the scaling factor (SF) is the time in seconds that each leaf viewing a target would need to be open to deliver the prescribed dose. The SF is patient-specific and is used to calculate the rotational period of the gantry, and the total treatment time (TTT) of the HT. The SF is generally difficult to estimate. Currently, it takes about one hour to fully optimize a prostate HT plan and to calculate the corresponding TTT. The aim of this study is to develop a method for estimation of the SF directly using a patient-specific approximating function. **Materials and Methods:** The SFs of ten randomly selected patients were used to build the approximation model. For the entire group of patients the PTV₁ ranged from 57 to 396 cm³ for PTV₁ margins from 2 to 10 mm. The discrete data for every patient is represented by an individual function, $SF=f(k \times PTV_1)$. The values of the function were rescaled to a special unit which represents the target volume irradiated with the prescribed dose per second. The values were normalized with two "geometric" parameters, namely, the target-to-target and the body-to-body ratios. After the normalization, the function for every patient was ordered in the file by the volume of the prostate and seminal vesicles. **Results:** For prostate HT planning, it was found that the planning target volume (PTV₁) has a higher impact on the SF values than the size of the patient's bodies. The function $SF=f(k \times PTV_1)$ was found smooth and continuous over the given interval. The rescaled and normalized functions for all patients were represented as delimiters of a 2D field. **Conclusion:** The method proposed for determination of the SF and TTT for HT prostate planning covers PTV₁ of four margins and a volume of prostate and seminal vesicles ranging from 42.8 to 161 cm³. Using these approximations, the TTTs for a second group of patients were determined in several minutes with deviation ranging from -2.8% to +7.1% compared to that of the TTTs calculated using the HT planning system. *Iran. J. Radiat. Res., 2010; 7 (4): 177-185*

Keywords: Helical tomotherapy, prostate treatment, scaling factor.

INTRODUCTION

In the last several years, Helical

Tomotherapy (HT) has been used to treat different cancers by providing conformal dose coverage at the planning target volume (PTV), while sparing the surrounding organs at risk (OAR) (1-9). HT converts the modulated fluence distribution to a map of pencil beams, where each beam delivers a discrete dose portion to the tumour using an individual level of fluence modulation. For a given dose rate, beam output and target dimensions, the optimized distribution can be delivered for a specific total treatment time (TTT). According to the manufacturer, the time can be determined using equations 1 and 2:

$$TTT = (NAP \times RP) / (PPR \times 60), [\text{min}] \quad (1)$$

$$RP = (SF \times MF \times D_f \times PPR) / D_{pr}. [\text{s}] \quad (2)$$

The factors in these equations are explained next. NAP is the number of activated projections per treatment. As the tumour is treated longitudinally, NAPs can be calculated from the target length, treatment pitch (p), beam width (BW) and the projections per rotation (PPR). The PPR is fixed by the manufacturer, i.e. PPR = 51. RP is the rotational period of the gantry. D_f is the dose per fraction and D_{pr} is the prescribed dose. The SF is the time that each leaf viewing a target would need to be open to deliver the prescribed dose and, as such, takes the machine output, target and patient size into account. It is patient-specific, and for a given beam setup, the SF depends on the target and patient size. MF

*Corresponding author:

Dr. Grigor Grigorov,
Medical Physics Department, Grand River Regional
Cancer Center, PO Box 9056, 835 King St West,
Kitchener, ON, N2G 1G3, Canada.
E-mail: grigorovgn@yahoo.ca

is the modulation factor, which presents the modulation of the beam intensity for a given SF. The MF associated with the beam output represents the ratio between the maximum and mean leaf opening time for all binary leaves that are open in a projection. A greater MF and smaller p and BW imply a greater number of intensity levels and number of activated beams resulting in better dose delivery⁽¹⁰⁻¹¹⁾. However, the decrease of the p and BW values may significantly prolong the treatment time and that may cause a reduction of the treatment quality due to the patient motion. For prostate HT, it was experimentally determined that $p = 0.5$ and $BW = 25$ mm lead to a reasonable dose distribution and TTT⁽⁴⁾.

The SF, however, is a parameter difficult to estimate, and is normally not available to the planner until the treatment plan is complete. The RP used for a particular treatment can be calculated using equation 2 with (1) the dose delivered to the target per fraction, (2) the prescription dose, (3) the MF and (4) the SF, which is available from the planning system. If the dose distribution and the dose-volume histogram (DVH) control points and/or the TTT are not acceptable, the plan needs to be re-optimized using a new planning setup⁽⁶⁾. Currently, it takes about one hour to fully optimize a prostate HT plan, check the dose distribution, and calculate the corresponding treatment time. Therefore, an *a priori* method for estimation of the SF and, consequently, the TTT may reduce the time for the plan optimization. To calculate the SF independently, without the HT planning system, it is possible to use mathematical models for estimation. If enough statistical data is collected from real plans, multi-parameter interpolation techniques can be applied, and the resulting approximations will be within reasonable error margins.

In this study we propose a method for the estimation of the SF directly, using a specific 2D field for approximation. In the field, the data for every patient is represented by an individual linear func-

tion, $SF = f(k \times PTV_1)$ of different slope. To order the functions in the field according to the volumes of the patients' prostates and seminal vesicles, rescaling and normalization of the functions were used. The values of the function were rescaled to a special unit which represents the target volume irradiated with the prescribed dose per second. The values were normalized with two "geometric" parameters, namely, the target-to-target and the body-to-body ratios. The SFs of ten randomly selected patients were used to build the approximation fields, for PTV margins ranging from 2 to 10 mm. A second group of ten patients was used to verify the method. The TTTs for a margin of 10 mm and a fractional dose of 2 Gy/fx were determined in several minutes. The deviation of the TTT values ranged from -2.8% to +7.1% compared to the TTTs calculated using the HT planning system.

MATERIALS AND METHODS

Prostate patients and HT planning

The CT scans of ten patients with T1-T3 staged prostate cancers were used in the treatment planning for HT. A single clinician contoured the patients' gross target volumes (GTVs) and the critical organs in the CT studies. The OAR and 3D uniform target contours were outlined for each patient according to the guidelines of the RTOG P-0126 protocol⁽¹²⁾. Two PTVs were used: PTV_1 includes both the seminal vesicles and the prostate, and PTV_2 includes the prostate only. To study how the SF depends on the sizes of the target and the patient, 3D uniform margins of 2, 5, 7.5 and 10 mm were generated. A variety of patient organ volumes were found: prostates from 38.9 to 148 cm³, seminal vesicles from 4.5 to 21.8 cm³, rectums from 38 to 277 cm³ and bladders from 52 to 292 cm³. The target volumes and normal structures were determined using the Picker (Phillips) AcQSim software. An escalated prescribed dose of 82 Gy (2 Gy/fx) was used in the planning.

The calculation of the dose distribution was done in software initially calibrated for a dose rate of 600 cGy min⁻¹. The calibration of the Tomotherapy unit was performed with a water phantom with a static field at depth = 5 cm, source-to-surface distance = 80 cm, source-to-axis distance = 85 cm, in the configuration where BW = 5 cm, the gantry is not rotating (i.e. gantry angle = 0) and the couch does not move (i.e. $p = 0$). This study used the configuration of $p = 0.5$ and BW = 25 mm which is recommended for prostate cancer⁽⁴⁾. The patients' plans for margins from 2 to 10 mm were optimized using the factors of precedence, importance and penalties, establishing a class solution for a template HT planning of prostate (see table 1). Two "geometric" normalizing ratios, namely, the body-body ratio (BBR) and the target-to-target, or prostate-seminal vesicle ratio (PSR) were defined. The BBR is the ratio of the average distance of the patient body from the isocenter to the patient surface to the maximum average distance of 13.5 cm measured in the used patient population. The distances were measured for 51 gantry positions starting from 0 deg and with a step of 7 deg. The PSR is the ratio of the volume of the prostate and seminal vesicles for each patient, to the maximum prostate and seminal vesicle volume (161 cm³) registered in the used patient population. In our patient group, the BBR and PSR were in the range from 1 to 0.811, and from 1 to 0.266, respectively. Picker (Philips) AcQSim software was used to calculate for every patient the average

distance and the length of the PTV₁. It is important to note that to calculate the shortest treatment times (smallest SF and RP), all plans were initially optimized for MF = 1. Then the MF was increased by a step of 0.01, and the plan was re-optimized so as to achieve the best combination of MF and SF and to satisfy the dose control point of the critical organs prescribed in protocol RTOG P-0126⁽¹²⁾. It was adjusted for the entire patient group using multiple (over 800) re-optimizations including the full dose calculation. Typical transversal/coronal/sagittal dose distributions and DVHs for one patient in the group are shown in figure 1. The plan in the figure was optimized for a margin of 7.5 mm and a treatment dose of 82 Gy. A TTT of 3.91 minutes was calculated for MF = 1.21, RP = 20 s, $p = 0.5$, BW = 25 mm and NAP = 599. Almost one hour was used to optimize one HT plan and to calculate of the SF and the TTT using the documentation from the manufacturer⁽¹³⁾.

Dependence of the SF on the body and PTV₁ sizes

The SF depends on the dose rate (DR), the beam setup, the patient's body and target sizes. As the DR is number of pulses, or monitor units per time, it is possible to assume that the SF depends linearly and inverse proportionally on the DR. Therefore in this study we do not investigate the dependence of the SF on the DR.

For the entire group of patient, the SF is plotted against the PTV margin in figure 2(a). The curves have linear character and

Table 1. Template objectives and constraints for the prostate HT optimization.

Targets	Importance	Max D Pen.	Min D Pen.	Max D [Gy]	Min D [Gy]	DVH D [Gy]	DVH-Vol [%]
PTV ₁	120	2000	2200	83	81	82	95
PTV ₂	50	20	1000	59	57	58	95
OAR	Importance	Max D [Gy]	Max D Pen.	DVH D [Gy]	DVH Vol [%]	DVH Pt. Pen.	-
Rectum	20	60	20	30	20	80	-
Bladder	10	60	10	30	20	5	-
Femurs	10	40	10	30	20	5	-

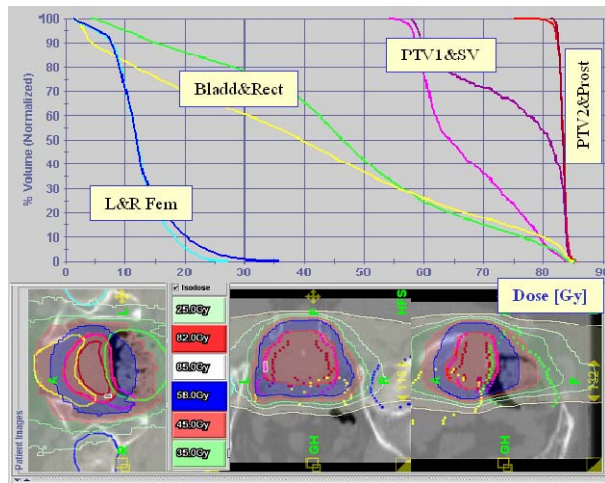


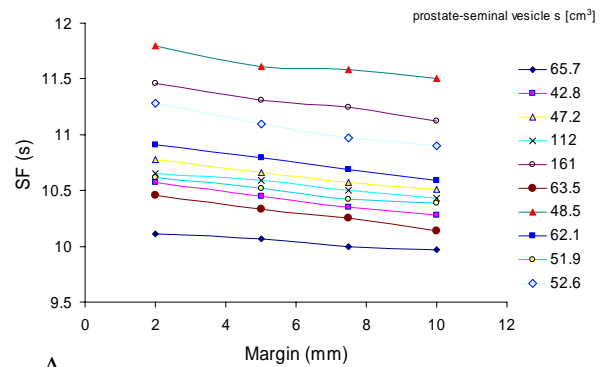
Figure 1. A typical HT plan for a prostate patient. The transversal/coronal/sagittal dose distribution was taken from the isocenter of the target. The PTV_{1,2} margins are 7.5 mm. The plan is optimized for a treatment dose of 82 Gy. The doses of the DVH control points satisfy the prescriptions of the RTOG-0126 protocol.

similar slope. After the normalization of the patients' SFs with the corresponding BBR and PSR, the curves in the figure were ordered according to the target volume, as shown in figure 2(b). The dependence of the SF on the PTV₁ volume is plotted in figure 3. In the figure, the initial SFs and their normalization with the BBR and PSR are plotted with circles, squares and triangles, respectively. The values of the SF in figure 3 are for PTV₁ = 10 mm, BW = 25 mm and $p = 0.5$ mm. Similar tendencies were found for other combinations of these parameters.

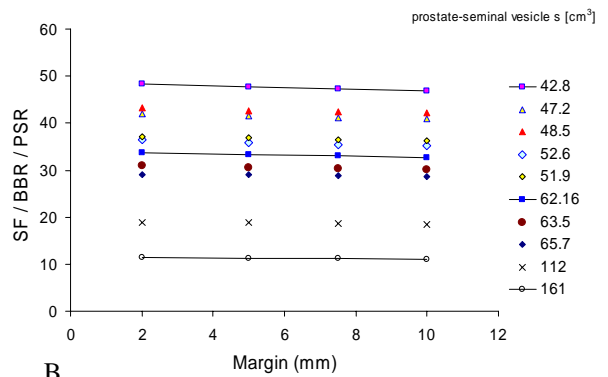
Determination of the SF

In figure 3, it can be seen that the PSR has a significantly higher impact on the SF values than the patient's body size (see the dependence plotted in triangles). Thus, PTV₁ instead of PTV₂ was used in the study because PTV₁ includes both the prostate and the seminal vesicles.

The discrete SF values, calculated using the HT planning workstation, are plotted against the PTV₁ in figure 4. The dependence $SF = f(PTV_1)$ is shown for BW = 25 mm and $p = 0.3, 0.5$ and 0.6 in circles, triangles and squares, respectively. The discrete SF values show a slightly increasing tendency as the PTV₁ increases. The



A



B

Figure 2. Dependences of the SF on the margin: (A) original SF and (B) rescaled SF.

determination of the SF for a new patient directly from figure 4 would not be accurate. In figure 4, the interpolation linear series for the plans with a 10 mm margin (black circles in figure 4), for example, have a small slope and significant data scatter. As the function $SF = f(PTV_1)$ is insufficient to establish an accurate estimation of the SF, our goal is to find the dependence $SF = f(k \times PTV_1)$, where k is a correction parameter related to the absolute target volume, and "geometric" normalization factors. The dependence requires the following two steps: rescaling and normalization of the discrete values:

1) Rescaling of every SF by its corresponding target volume:

$$Y_1 = PTV_1 / SF, [cm^3/s] \quad (3)$$

Y_1 represents how much volume of the PTV₁ (in cm³) can be irradiated per unit time with the $D_f = 2$ Gy/fx. If a different fractional dose, D_x , is used, the factor (D_x/D_f) must be applied in equation 2. The values of Y_1 are plotted in figure 5 for the same BW and p as

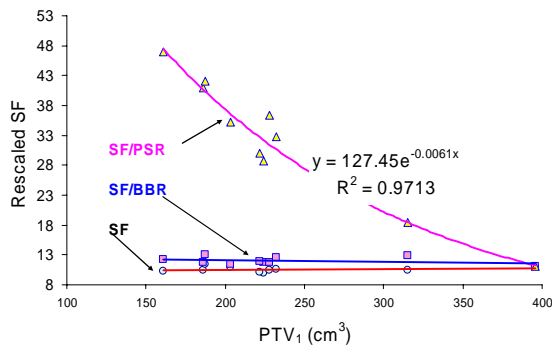


Figure 3. Comparison between the original SF and the rescaled SF with the PSR and BBR ratios. The values of the SF in the figure are calculated for 10 patients using $PTV_1 = 10$ mm, $BW = 25$ mm and $p = 0.5$ mm.

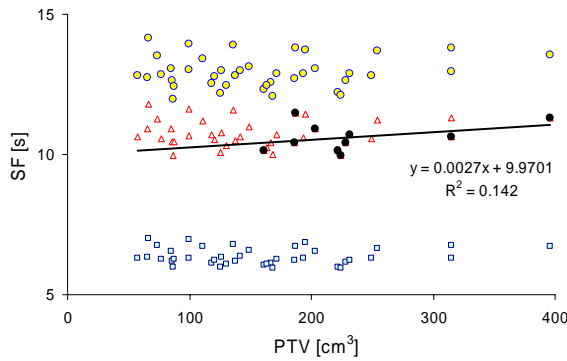


Figure 4. The function $SF = f(PTV_1)$ for $BW = 25$ mm. In the figure, the SFs of 40 plans for $p = 0.3, 0.5$ and 0.6 (in circles, triangles and squares, respectively) are included. The interpolation curve is for $BW = 25$ mm, $p = 0.5$ and margin = 10 mm.

in figure 4. For a given PTV_1 , the rescaled functions Y_1 allow for more accurate determination of the SF. The new function is fitted to a linear series with $R^2 \approx 0.99$ (see figure 5). However, the combination of a small prostate volume with bigger margin may result in the same PTV_1 and Y_1 as for a small margin with larger prostate volume. Some combinations of the target volume and patient's body size may produce a similar effect.

In figures 4 and 5, three groups of discrete values of the SFs and functions Y_1 are plotted, respectively. Every group includes the values of 10 individual plans (patients) optimized for four PTV margins (2 to 10 mm) and three values of p (0.3, 0.5 and 0.6).

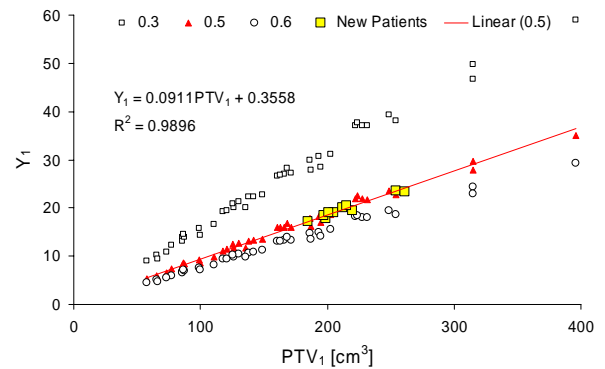


Figure 5. Function Y_1 represents the rescaled SF using Eq. 3. Parameters are the treatment p (0.3, 0.5 and 0.6).

2) Normalization of the SF using the BBR and PSR ratios:

$$Y_2 = Y_1 / (PSR \times BBR), [cm^3/s] \quad (4)$$

Figure 6 shows the normalized functions Y_2 for our group of patients. The functions are ordered according to the volumes of the prostate and the seminal vesicles. Every function has four values determined by the different PTV margins. The distribution of the Y_2 functions in the plot form a 2D field. This field can conveniently be used to approximate the SF for a new patient. In figure 6, the curves represent the patients' specific ranges of the SF for a margin from 2 to 10 mm, and for prostate- seminal vesicle (PS) volume from 42.8 to 161 cm^3 . In the figure, lines are used to connect the Y_2 points with the same margins for patients with different PS volumes. The black lines correspond to different PTV margins: the "solid", "dashed", "dashed with one point" and "dashed with two point lines" are for margins of 10, 7.5, 5 and 2 mm, respectively. The lines in pink, red, blue and orange are for the prostate and seminal vesicle volumes equal to 42.8, 62.1, 112 and 161 cm^3 , respectively. The curve with the greatest slope represents the smallest PS volume of 42.8 cm^3 , and the curve with the smallest slope represents the largest PS volume of 161 cm^3 .

The SF for a new patient of known PS volume can be calculated using Y_2 , PSR,

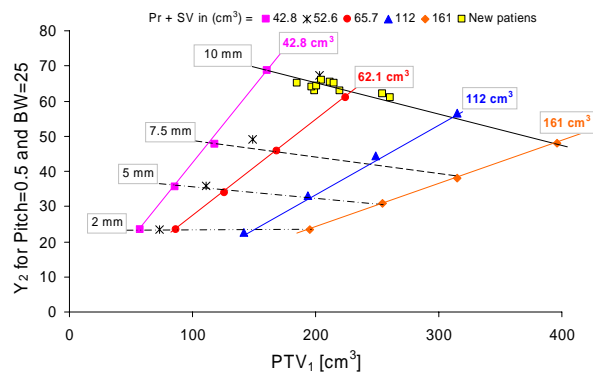


Figure 6. The 2D field for a direct estimation of the SF using Eq. 5. The values of function Y_2 are given for $D_f = 2$ Gy, $p = 0.5$ and $BW = 25$ mm. Each line contains four data points which correspond to different PTV margins (ranging from 2 to 10 mm). Solid, dashed, dashed with one point and dashed with two points lines are for margins equal to 10, 7.5, 5 and 2 mm, respectively. The pink, red, blue and orange lines are for the prostate and seminal vesicle volumes equal to 42.8, 62.1, 112 and 161 cm^3 , respectively.

BBR and PTV_1 based on equation 5:

$$SF = k \times PTV_1 [s],$$

where $k = 1 / (Y_2 \times PSR \times BBR)$ (5)

Calculation of the NAP

To calculate the TTT, we need the number of activated projections. The NAP depends on the target length (PTV_1), BW , p and PPR. The PPR = 51 projections; this is fixed by the manufacturer. For example, assuming a $BW = 2.5$ cm, $p = 0.5$, target length = 10 cm, and considering that the treatment covers a target length plus a BW above and beyond ($10 + 2 \times 2.5$ cm = 15 cm), the total number is $51 \times 15/2.5/0.5 = 612$ activated projections.

Estimation of the TTT

The methodology was verified using a second group of ten patients with medium prostate and seminal vesicle volumes. The corresponding TTTs for a 10 mm margin were determined with $BW = 25$ mm and $p = 0.5$ using the SF and NAP as described in Sections 2.3 and 2.4. The HT plans of the new patients were optimized using the same beam setup as in Section 2.1. The Y_1 and Y_2 values of the new patients are plotted in figures 5 and 6, respectively. The TTT

values calculated by both techniques are shown in figure 7, where the TTTs obtained with the HT planning system are in circles, and the values calculated with the new method are in squares.

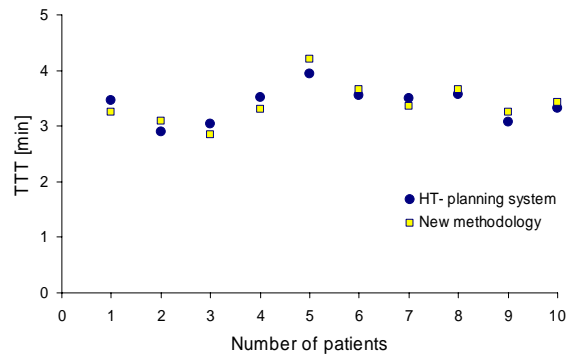


Figure 7. A comparison between the TTTs calculated by HT planning system, in circles, and the new method, in squares.

RESULTS

This study used the class solution for HT prostate planning as shown in table 1. Overall, the DVH prescriptions and control points for the PTV margins from 2 to 7.5 mm were well satisfied (12). Several prescribed DVH control points for 15% of the rectum and bladder were not satisfied. For all plans, the prescribed doses for PTV_1 and PTV_2 , for 1%, 95% and 99% of the PTVs were very well satisfied. Hot regions in the PTV_2 were not found, and the dose for $PTV_2 \leq 87.1$ Gy.

Figure 2(a) shows the discrete values of the SF plotted against the used PTV margin. In the figure, $BW = 25$ mm, $p = 0.5$ and $D_f = 2$ Gy. In figure 2(a), the curves for the patients are labelled with the corresponding prostate and seminal vesicle volumes. Each curve has an almost constant slope. As plotted in figure 2(b), after the normalization with the BBR and PSR ratios, the curves are ordered from the largest to the smallest prostate and seminal vesicle volume. The larger SF for the smaller targets can be explained by the reduced beam output. Figure 3 has three plots. The SFs in circles are obtained using HT

planning system. The rescaled values are also plotted, in squares for BBR and in triangles for PSR. The PSR has a significantly higher impact on the SF values than the patient's body size. The interpolation function for the 10 mm margin fits very well to a curve given by a power series with $R^2 > 0.9$.

The methodology was tested using a second group of 10 patients with medium prostate and seminal vesicle volumes. The average PTV_1 , BBR, PSR, SF, MF and TTT of the second population are shown in table 2. For the entire group of patients, TTTs in the range of 2.9 to 4.2 minutes were estimated, for a 10 mm margin with $RP = 20$ s, $MF = 1.3$ to 1.5 , $p = 0.5$ and $BW = 25$ mm.

A comparison between the TTT values calculated using the HT planning system and the proposed approach is plotted in figure 7. Differences of -2.8% to $+7.1\%$ were observed.

Table 2. Parameters for the second group of prostate Patients.

	PTV_1 [cm ³]	P-SV [cm ³]	SF [s]	MF	NAP
min	185	45	10.2	1.41	444
max	261	72.4	11.3	1.57	603
aver	215	57.1	10.7	1.5	518
SD	26.6	8.6	0.37	0.052	47.2

DISCUSSION

This is the first work on the estimation of the SF for HT using 2D approximating fields, which has not been published so far. According to the acquired data associated with the related normalization factors and equations, we propose a novel method to estimate the SF and TTT for the prostate HT. The method uses a 2D field with two ranges, one for the PTV_1 margin and the other for the volume of the prostate and the seminal vesicles. The definition of the field is based on the use of an original concept of rescaling and normalization of the SFs obtained from the HT planning for ten randomly selected prostate patients. The method is verified by a calculation of the SF

for a second group of ten prostate patients.

According to the results of the first phase of this investigation (figures 2 – 6) and results of the verification phase of the TTT for the second group of prostate patients (figure 7), it is seen that the approximating 2D field to determine the SF for the prostate HT patients using equation 6 is generally acceptable. Considering the results of these phases, it can be realized that the range of SF difference (from -2.8% to $+7.1\%$) used to determine the total treatment time for prostate Tomotherapy treatment is reasonable⁽⁴⁾. The methodology for the derivation of the 2D field for a direct estimation of SF was presented step by step (see figures 4 – 6 and equation 3 – 5).

The main contribution of this study is to show how to use the multi-parametrical depending discrete values ($SF \propto$ (body and beam parameters)) to build up a simple functional dependence ($SF = k \cdot PTV_1$) using normalization factors ($k = (Y_2 \cdot PSR \cdot BBR)^{-1}$).

The most important factors contributing to the 2D approximating field are as follows:

1. The SF depends on the beam setup, patient's body and target size. For the entire group of patient, the SF is plotted against the PTV margin in figure 2(a) having linear character and similar slope.
2. After the normalization of the patients' SFs with the corresponding BBR and PSR, the curves in the figure were ordered according to the target volume, as shown in figure 2(b). This allows determining the SF for a new patient using an approximation for the given target volume.
3. It was found that the PSR has higher impact than BBR. In figure 3, the dependence of the SF on the PTV_1 normalized with PSR is plotted with triangles and can be substituted by an exponential equation, $R^2 = 0.97$.
4. The function $SF = f(k \cdot PTV_1)$ is smooth

- and continuous over the given interval.
- The method for determination of the SF and TTT for HT prostate planning covers PTV₁ ranging from 57 to 396 cm³. By using an interpolation technique, the SFs for other targets (patients) can be estimated using figure 6 and Equation 5.
 - The 2D field plotted in figure 6 is constructed for a fractional dose of 2 Gy/ fx, $p = 0.5$ and BW = 25 mm, for BBR = 1 to 0.811, PSR = 1 to 0.266 and for prostate and seminal vesicle volumes from 42.8 to 161 cm³. The grid in figure 6 makes the interpolation easier for a given PS volume and PTV margin. The black lines are for margins. The colour lines in the figure are for prostate and seminal vesicle volumes. If higher or lower pitch is used, we assume that the slope of the curves for the patients shown in figure 4 will be smaller or bigger, respectively. The effect of change in the BW should be similar. For different p and BW, the NAP will be inversely proportional. And
 - Using the new method, the calculation of the TTTs for the whole second group of patients took several minutes, while in the planning system⁽¹³⁾ it took more than an hour per patient.
 - The high dose ⁽¹²⁾ template HT prostate planning was well satisfied for the PTV margins from 2 to 7.5 mm. For a PTV margin of 10 mm, several prescribed DVH control points for 15% of the rectum and bladder were not satisfied. This can increase the rectal and bladder toxicity.

The new HiArt machines and software versions may allow using a finer tuning patient-to-patient of the BW, p and MF. As the dependence of the SF on these parameters was found to be smooth and none interrupted, we believe that the proposed method can be used to estimate the SF, MF and TTT for other tumour sites in all the possible spectrum of the beam and plan optimization parameters. A library of

the SF function and its factors (p , BW, PSR, BBR, margin, PTV₁, MF and Y₂) can be built for different types of tumours. The method can also be extended and improved using better patient statistics. The clinical impact of the proposed method is related to the ability to estimate the individual SF and TTT based on the fractional dose, PTV margin and the prostate and seminal vesicle volume before the HT planning.

CONCLUSION

This study proposed a novel method to estimate the SF for prostate HT using a 2D field. This approach can be used as an alternative to the use of HT planning system for the calculation of TTT. Although this study used a population of only ten patients, the results are acceptable. The function $SF = f(k \times PTV_1)$ is smooth and continuous over the given interval. The method for determination of the SF and TTT for HT prostate planning covers PTV₁s of four margins and a volume of prostate and seminal vesicles ranging from 42.8 to 161 cm³. By using an interpolation technique, the SFs for other targets (patients) can be estimated using figure 6 and equation 5. The relatively short time taken to obtain the SF and TTT makes the proposed method a clinically useful tool.

ACKNOWLEDGEMENT

The London Regional Cancer Program, London, Ontario, Canada, the Ontario Cancer Research Network, and the Ontario Research and Development Challenge supported this research. As former employees at the LRCP, both authors have special thanks to Tomas Kron, Glenn Bauman, George Rodrigues, Jerry Battista and Jake Van Dyk.

REFERENCES

- Mackie TR, Holmes TW, Swerdloff S, Reckwerdt P, Deasy JO, Yang J, Paliwal B, Kinsella T (1993) Tomotherapy: a

- new concept for the delivery of conformal radiotherapy. *Med Phys*, **20**:1709–1719.
2. Mackie TR, Olivera GH, Reckwerdt PJ, DM Shepard (2000) Convolution/superposition photon dose calculation, *General Practice of Radiation Oncology Physics in the 21st Century* ed A S Shui and D EMellenberg (Madison WI: Medical Physics Publishing) 39–56 (Published for AAPM).
 3. Shepard DM, Olivera GH, Reckwerdt PJ , Mackie TR (2000) Iterative approaches to dose optimization in tomotherapy. *Phys Med Biol*, **45**: 69–90.
 4. Grigorov GN, Kron T, Wong E, Chen J, Sollazzo J, Rodrigues G (2003) Optimization of helical tomotherapy treatment plans for prostate cancer. *Phys Med Biol*, **48**: 1933–1943.
 5. Van Dyk J (2003) Early experience with helical tomotherapy, 7th Biennial European Society of Therapeutic Radiation Oncology, Annual meeting on physics and radiation technology for clinical radiotherapy. Geneva, Switzerland; 13–18 .
 6. Kron T, Grigorov GN, Yu E, Yartsev S, Yartzev S, Chen J, Wong E, Rodrigues G, Trenka K, Coad T, Bauman G , Van Dyk J (2004) Planning evaluation of radiotherapy for complex lung cancer cases using helical tomotherapy. *Phys Med Biol*, **49**: 3675–3690.
 7. Gladwish A, Kron T, McNiven A, Bauman G , Van Dyk J (2004) Asymmetric fan beams for improvement of the craniocaudal dose distribution in helical tomotherapy delivery. *Med Phys*, **31**: 2443–2448.
 8. Fiorino C, Dell'Oca I, Pierelli A, Broggi S, Martin E, Muzio N, Longobardi B, Fazio F , Calandrino R (2006) Significant improvement in normal tissue sparing and target coverage for head and neck cancer by means of helical tomotherapy. *Radiother Oncol*, **78**: 276–282.
 9. Mackie TR (2006) History of tomotherapy. *Phys Med Biol*, **51**: R427–R453.
 10. Welsh JS, Lock M, Harari PM, Tome WA, Fowler J, Mackie TR, Ritter M, Kapatoes J, Forrest L, Chappell R, Paliwal B, Mehta MP (2006) Clinical implementation of adaptive helical tomotherapy: a unique approach to image-guided intensity modulated radiotherapy. *Technol Cancer Res Treat*, **5**: 465–479.
 11. Rodrigues G, Yartsev S, Chen J, Chen J, Wong E, Souza D, Lock M, Bauman G, Grigorov g, Kron T (2006) A comparison of prostate IMRT and helical tomotherapy class solutions. *Radiother Oncol*, **80**: 374–377.
 12. Michalski J, Purdy J, Bruner D, Amin M (1993) ICRU Report 50 Prescribing, Recording, and Reporting Photon Beam Therapy (Bethesda, MD: International Commission on Radiation Units and Measurements).
 13. TPGB-2002, Tomotherapy planning guide book.

